Central European Journal of Energetic Materials
ISSN 1733-7178; e-ISSN 2353-1843

Cent. Eur. J. Energ. Mater. 2019, *16*(3): 360-379; DOI 10.22211/cejem/112234
Article is available in PDF-format, in colour, at:
http://www.wydawnictwa.ipo.waw.pl/cejem/Vol-16-Number3-2019/CEJEM_00995.pdf

Research paper

Thermal Degradation Behaviour and Kinetics of aged TNT-based Melt Cast Composition B

Arjun Singh,[1*] **Tirupati Chander Sharma**,[1,2]
Vasundhara Singh,[2] **Niladri Mukherjee**[1]

[1] *Terminal Ballistics Research Laboratory, DRDO, Ministry of Defence, Explosive Group, Sector 30, Chandigarh (UT) – 160030, India*
[2] *Applied Sciences, Panjab Engineering College, University of Technology, Chandigarh – 160012, India*
[*] *E-mail:* arjunsngh@yahoo.com

Abstract: In the present paper, three kinds of aged and freshly prepared 2,4,6-trinitrotoluene (TNT) based Composition B stockpiled, for a period of 20 and 32 years, were investigated for the effect of natural ageing on their thermal degradation behaviour and kinetic parameters. The properties investigated indicated that there was no significant change in the thermal stability of the samples aged under natural environmental conditions. The kinetic parameters were studied by means of the Kissinger method using the peak temperature at maximum reaction rate from DSC data, and the isoconversional Kissinger-Akahira-Sunnose (KAS) and ASTM E689 methods from TGA data. The apparent activation energies calculated by the Kissinger method were 173.8 kJ·mol^{-1} for fresh, 170.4 kJ·mol^{-1} for 20 y old and 187.1 kJ·mol^{-1} for 32 y old Composition B, respectively. The values calculated by the KAS method were found to be in the range 77.2-235.8 kJ·mol^{-1} for fresh Composition B, 75.7-224.0 kJ·mol^{-1} for 20 y old and 70.4-196.0 kJ·mol^{-1} for 30 y old Composition B, respectively. The activation energies obtained from the KAS methods are in good agreement and consistent with the isoconversional ASTM E689 kinetic method. The thermodynamic parameters, such the Gibbs free energy of activation ($\Delta G^{\#}$), activation enthalpy ($\Delta H^{\#}$) and activation entropy ($\Delta S^{\#}$) for the formation of activated complexes were also studied and are discussed.

Keywords: Composition B, thermal degradation, thermogravimetry, Differential Scanning Calorimetry, kinetics, thermodynamic parameters

1 Introduction

Common energetic compounds such as 2,4,6-trinitrotoluene (TNT), 1,3,5-trinitro-1,3,5-triazacyclohexane (RDX), 1,3,5,7-tetranitro-1,3,5,7-tetrazocine (HMX) *etc.* Are most widely used for the manufacture of bombs, artillery shells, and warhead fillings in military applications [1]. TNT-based melt-cast explosive formulations have been widely developed in industrial and military applications because of their high energy content, high power performance, high detonation velocity and adjustability to various shapes *etc.* [2, 3]. For example, Composition B (RDX/TNT) and Octol (HMX/TNT) are the most popular formulations that are still used on a large scale as the main explosive charges in munitions. TNT has the advantages of low cost, good chemical and thermal stability, compatibility with other energetic compounds, fairly high explosive power, a low melting point favourable for melt casting operations and moderate toxicity [4-6].

The most popular melt-cast explosive formulation is the so-called Composition B, which is made up of 60 wt.% of RDX and 40 wt.% of TNT. It is widely used as a military-grade explosive because of its outstanding physical properties, ease of manufacture and relatively high detonation power [4, 7, 8]. It has been extensively studied for its safety parameters in terms of thermal sensitivity, mechanical sensitivity and theoretical studies [9, 10]. These formulations, which are filled into warheads/munitions and projectiles, have a tendency to undergo slow degradation during storage under various conditions for many years. This phenomenon degrades the stability of the formulations, thereby resulting in poor performance and low service life. The degradation process may enhance the sensitivity which will be hazardous during transportation, handling and use [11, 12]. There are many studies reported in the literature which have described the ageing phenomena of energetic compounds and munitions/energetic formulations [13-17]. In thermal ageing, several energetic compounds and their formulations have been investigated at 70 °C with varying levels of humidity or without reporting the humidity. Many researchers have paid attention to the lifetime assessment of energetic compounds and their formulations for its direct association with storage safety and service life. A knowledge of the expected lifetime of various formulations is valuable information not only for safety and performance, but also for economic reasons. In the ageing process, the thermal degradation stability can lead to failure mode or accidental ignition during storage.

Thermal stability is generally studied by using several experimental techniques including thermogravimetry (TG), differential scanning calorimetry (DSC), one-dimensional time to explosion (ODTX), scaled thermal explosion (STEX) and accelerated rate calorimetry (ARC) [18-20]. Each of these experimental techniques has its different characteristics and requires a small amount of sample for reliable data acquisition which serves the safety of operation. These techniques have also been proven to be good tools for monitoring the ageing process of energetic compounds [21] and their formulations, including Composition B. In the present work, we propose to investigate the effect of the natural ageing process on the thermal properties of Composition B, which has been stored in the casing for 20 and 32 y under natural environmental conditions. It should also determine whether this composition could still be used for military application or should be destroyed.

In the present paper, the thermal degradation behaviour and kinetic parameters were investigated through the Kissinger method from DSC data, and the isoconversional Kissinger-Akahira-Sunnose (KAS) and ASTM E689 methods from TG data. The thermodynamic parameters, including the Gibbs free energy of activation ($\Delta G^{\#}$), activation of enthalpy ($\Delta H^{\#}$) and activation of entropy ($\Delta S^{\#}$) for the formation of activated complexes were also studied and are discussed.

2 Experimental

2.1 Materials

Composition B formulations which had been stored for 20 and 32 y in a magazine was used for the thermal degradation studies. This formulation was exposed to and was in direct contact with the casing under natural environmental conditions. The temperature and humidity of storage were in the range 4-47 °C and 40-95% RH, respectively. A fresh batch of Composition B was also prepared from RDX and TNT for the thermal degradation behaviour and kinetic parameters studies. These formulations were abbreviated as RT_1 for fresh Composition B, RT_2 for 20 y and RT_3 for 32 y stored Composition B, respectively.

2.2 Characterization

Non-isothermal thermo-gravimetric (TG) and its derivative thermo-gravimetric (DGT) analysis were performed using a Mettler Toledo Thermogravimetry/Differential scanning calorimetry (TGA/DSC 1 Star System). A sample mass of approximately 5 ±1.0 mg was placed in a standard 70 μL

uncovered alumina crucible where the sample was subjected to heating from 25-400 °C at different heating rates (2, 5, 10 and 20 °C·min^{-1}) under a nitrogen atmosphere. The flow rate of nitrogen gas was kept constant at 30 mL·min^{-1}. The collected thermal data were used for calculation of the kinetic parameters by means of different kinetic methods.

2.3 Kinetic analysis

According to non-isothermal kinetic theory of heterogeneous solid-gas processes, the rate of reaction is the product of two variable functions, one depending solely on the temperature (T), and the other depending solely on the extent of conversion (α), by the well-known Equation 1:

$$Rate = \frac{d\alpha}{dt} = k(T)\, f(\alpha) \tag{1}$$

where $\alpha = \frac{m_o - m_f}{m_o - m_\infty}$, m_t is the mass of the sample at time t, m_o and m_∞ are the masses of the sample at the beginning and the end of the degradation reaction, respectively. The temperature dependence of the process rate which is represented by the rate constant $k(T)$, is generally assumed to be given by the Arrhenius equation [22], shown in Equation 2:

$$k(T) = A \exp.\left(-\frac{E_a}{RT}\right) \tag{2}$$

where A is the pre-exponential factor, E_a is the activation energy (kJ·mol^{-1}). T is the absolute temperature (K) and R is the gas constant (8.314 J·(mol·K)$^{-1}$). The extent of conversion, the dependence of which is related to the experimental data, is illustrated by the differential reaction model, f(α). For dynamic data obtained at a constant heating rate, $\phi = dT/dt$, the new term and $k(T)$ are inserted in Equation 1 to give the following Equation 3:

$$\frac{d\alpha}{dT} = \frac{A}{\phi} \exp\left(-\frac{E_a}{RT}\right) f(\alpha) \tag{3}$$

For simple reactions, the evaluation of f(α) is possible with an elementary model function. For complex reactions, the functions of f(α) are complicated and generally unknown.

For kinetic parameter evaluation, the Kissinger method [23] represents a simple calculation method based on an assumption that the peak temperature for maximum mass loss changes with changes in the heating rate. Kissinger further

assumed that the mentioned change depends only on the activation energy value for the given reaction. This method may also be used to calculate the kinetic parameters of solid state reactions without prior knowledge of the reaction mechanism and reaction order by using Equation 4:

$$\ln\left(\frac{\phi}{{T_{max}}^2}\right) = \ln\left(\frac{AR}{E_a}\right) - \frac{E_a}{RT_{max}} \tag{4}$$

where ϕ corresponds to the heating rate, T_{max} is the peak temperature for maximum mass loss in Kelvin (K), and E_a is the activation energy (kJ·mol^{-1}). This equation is of linear form in which $\ln[\phi/(T_{max})^2]$ and $1/T_{max}$ are two variables from which the activation energy can be obtained easily from the slope of $\ln[\phi/(T_{max})^2]$ *versus* $1/T_{max}$ plots. It is interesting to note that the Kissinger method, although initially developed for first-order reaction, holds good for any kinetic model.

2.4 Isoconversional (model-free) method

Isoconversional methods are the most reliable for the calculation of kinetic parameters at different extents of conversion of thermal decomposition reactions without evaluating any particular form of the reaction model. The Kissinger-Akahira-Sunnose (KAS) isoconversional method [24] is presently used here to determine the kinetic parameters. The KAS is an integral isoconversional method, which is based on the Muaray and White approximation for the temperature integral as given by the following Equation 5:

$$ln\frac{\phi}{T_\alpha^2} = \ln\frac{AR}{E_a\, g(\alpha)} - \frac{E_a}{RT_\alpha} \tag{5}$$

where $g(\alpha)$ is the integral reaction model which is reported in the literature [24-26]. The activation energy for constant conversion is determined from the linear slope of $\ln(\phi/T_\alpha^2)$ *versus* $1/T_\alpha$ at different heating rates.

3 Results and Discussion

3.1 DSC study

Figure 1(a) shows the DSC curves of fresh Composition B at heating rates of 2, 5, 10 and 20 °C·min^{-1} under a nitrogen atmosphere. The DSC curves exhibited sharp endothermic and exothermic peaks corresponding to melting

and thermal degradation, respectively. The first endothermic peak was around 80 °C, which corresponds to the melting point (T_m). The single exothermic peak appeared in the range 215-242 °C at different heating rates due to the thermal degradation of RDX. In addition, the DSC measurements showed a broad steep endothermic peak between the endothermic peak of melting and the exothermic peak of thermal degradation, which corresponds to an evaporation process. This evaporation process can be observed as a special case of a zero-order process where the rate of evaporation depends on the temperature.

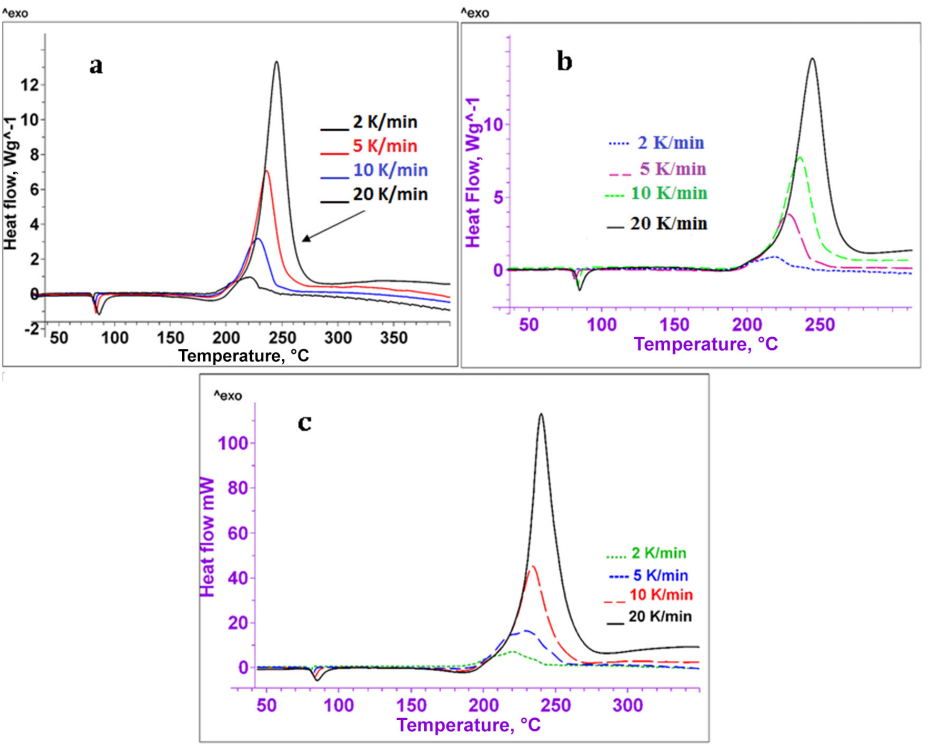

Figure 1. DSC curves of (a) RT_1, (b) RT_2 and (c) RT_3 samples obtained for different heating rates under nitrogen atmosphere

The thermal degradation behaviour of aged samples was also investigated by non-isothermal DSC under the same experimental conditions and compared with a fresh sample. Figures 1(b) and 1(c) shows the DSC curves for RT_2 and RT_3 samples, respectively. These showed similar endothermic and exothermic peaks corresponds to the melting, evaporation and degradation processes as observed for the RT_1 sample. There was no change in the endothermic

peak corresponds to melting, while the peak temperature for the exothermic peak appeared in the ranges 214-241 °C for RT_2 and 215-240 °C for RT_3 at different heating rate. The results also revealed that the peak temperature was either the same or exhibited an insignificant change for the aged samples. The initial degradation temperature (T_{onset}), the peak temperature at maximum reaction rate (T_{max}) and the termination of degradation temperature (T_{endset}) obtained from the DSC curves are listed in Table 1. The T_{onset} and T_{max} values shifted towards the upper range of temperatures with increasing heating rate. A similar effect of shift in the peak temperature has been reported by many researchers for different types of energetic compounds, including explosive formulations [25]. This indicates that the peak temperatures of the RT_2 and RT_3 samples are not changed significantly after prolonged natural ageing periods of 20 and 32 y, respectively, compared to that of a fresh sample.

Table 1. DSC data in terms of T_{onset}, T_{endset}, and T_{max} obtained at different heating rates under nitrogen atmosphere

Sample	Time [y]	ϕ [°C·min^{-1}]	Temperature [°C]		
			T_{onset}	T_{endset}	T_{max}
RT_1	0	2	184.4	223.5	215.9
		5	200.5	239.3	223.4
		10	211.4	247.4	232.2
		20	219.9	257.4	241.9
RT_2	20	2	193.7	226.6	214.6
		5	203.4	239.4	223.7
		10	210.7	247.2	232.5
		20	219.6	257.6	241.2
RT_3	32	2	195.8	228.9	214.9
		5	193.7	243.9	224.5
		10	209.8	248.1	230.5
		20	222.4	254.2	239.7

3.2 TGA study

The thermal degradation behaviour of fresh and aged Composition B was investigated for their mass loss profiles by the non-isothermal TG technique. The TG curves of RT_1, RT_2 and RT_3 samples obtained at different heating rates under a nitrogen atmosphere are shown in Figures 2(a) to 2(c). The TG curves showed that the mass loss could be attributed to a single stage due to the thermal degradation of TNT and RDX. A displacement of the thermal degradation

temperature in the TG curves was seen for all samples with increasing heating rate because the sample temperature lags behind that of the furnace temperature at high heating rates. The heat transfer from the furnace to the sample is accompanied with a delay process. The TG curves for RT_1 showed 6-10% mass residue at different heating rates, while it was found to be 8-11% for RT_2 and 11-18% for RT_3 samples. It was observed that the char residue for naturally aged RT_2 and RT_3 samples was slightly higher than for fresh RT_1 sample.

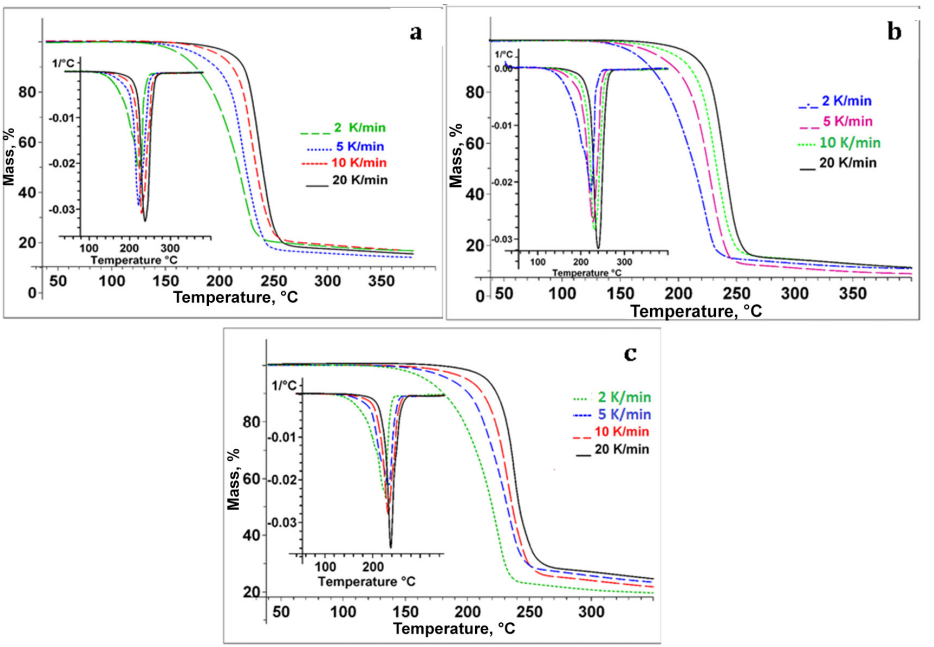

Figure 2. TG curves of (a) RT_1, (b) RT_2 and (c) RT_3 samples obtained for different heating rates under nitrogen atmosphere

Figures 2(a) to 2(c) also showed that the first DTG curves overlapped with the TG curves at different heating rates. They all showed a similarly accelerating vigorous progress that reached into a skewed maximum, and subsequently dropped to almost zero. As shown in Figure 2, the peak temperature values shifted towards a higher range of temperatures with increasing heating rates. The initial degradation temperature (T_{onset}), the temperature at maximum mass loss (T_{max}) and the termination of degradation temperature (T_{endset}), the three characteristic quantities along with residues of the RT_1, RT_2 and RT_3 samples, are listed in Table 2. The results showed that the T_{max} values of RT_1, RT_2 and RT_3 were 223.8, 225.0 and 228.9 °C, respectively, at a heating rate of 10 °C·min^{-1}. These T_{max} values

for all samples shifted towards a higher temperature with increasing heating rate. Similar, thermal degradation behaviour has been reported by many researchers and showed a similar trend of the peak temperature at the maximum mass loss with heating rate [27, 28]. The thermal stability of a fresh sample was found to be lower than that of the aged samples. This may be explained by the recent batch of TNT being more pure in this Composition B and thus has a higher freezing point and less thermal stability [29-31]. On the other hand, the ageing process may be performed on samples of TNT containing other derivatives, shifting the thermal degradation phenomena in an upwards direction. This means that the thermal stability of the aged samples is not reduced under natural environmental conditions during a prolonged natural ageing time of 32 y.

Table 2. TG data of T_{onset}, T_{endset}, and T_{max} along with residue (%) obtained at different heating rates from TG/DTG data

Sample	Time [y]	ϕ [°C·min^{-1}]	Temperature [°C]			Residue [%]
			T_{onset}	T_{endset}	T_{max}	
RT_1	0	2	187.5	227.4	216.0	10.1
		5	200.8	232.0	218.2	6.4
		10	210.9	239.7	223.8	8.3
		20	218.2	247.1	232.9	7.4
RT_2	20	2	186.7	225.6	218.2	10.8
		5	201.8	238.3	223.1	8.2
		10	210.1	241.0	225.0	11.0
		20	219.8	248.6	236.5	10.7
RT_3	32	2	193.5	226.9	221.2	11.4
		5	201.3	238.1	227.9	15.8
		10	211.7	241.3	228.9	14.1
		20	222.01	245.2	235.1	17.5

Figures 3(a) to 3(c) shows the progress of the thermal degradation in terms of the extent of conversion *versus* temperature at different heating rate. It was observed that there was no remarkable change in the mass loss up to 200 °C. Further increase in the temperature showed a vigorous change in mass loss, whereby their slopes increased with temperature and most samples became depleted at 200-250 °C. These results further exhibited a single step degradation process for all samples.

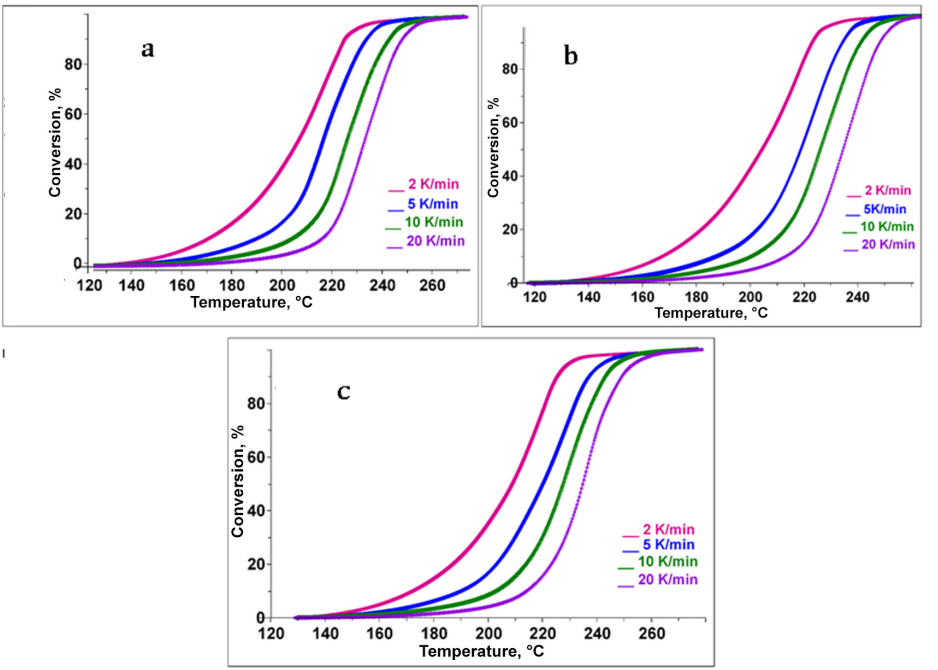

Figure 3. Dependence of conversion (percentage) *versus* temperature for (a) RT_1, (b) RT_2 and (c) RT_3 samples

3.3 Kinetic study

The Kissinger method was used for the investigation of the kinetic parameters for the thermal degradation from the DSC data. These kinetic parameters were calculated by the Kissinger equation (Equation 4) by plotting $\ln[\phi/(T_{max})^2]$ *versus* $1000/T_{max}$, as shown in Figure 4. The activation energy and pre-exponential factor (A) results, calculated from the slope and intercept respectively, are listed in Table 3. The results for the activation energies of RT_1, RT_2 and RT_3 were 173.8, 170.4 and 187.1 kJ·mol^{-1}, respectively. The main advantage of this method lies in its robustness with respect to data-distortive effects such as thermal gradients, inaccuracies of zero-line subtraction *etc*. However, the limitation of this method is that the reaction model function f(α) should not depend on the heating rate for calculation of the activation energy. It also enables a single activation energy value to be produced and does not describe an actual complex process. In a solid state reaction, a variation in the activation energy is observed for the elementary reaction due to a complex reaction mechanism. This variation can be investigated by means of the KAS isoconversional method.

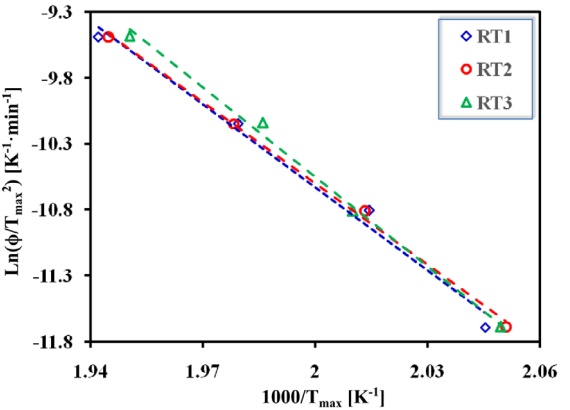

Figure 4. The Kissinger plots for RT_1, RT_2 and RT_3 samples obtained by the Kissinger method at different heating rates

Table 3. The activation energy and pre-exponential factor (A) of RT_1, RT_2 and RT_3 samples for the degradation reaction obtained by the Kissinger method using DSC data

Sample	E_a [kJ·mol^{-1}]	A [s^{-1}]	R^2
RT_1	173.8	$3.6 \cdot 10^{13}$	0.986
RT_2	170.4	$1.8 \cdot 10^{13}$	0.997
RT_3	187.1	$9.4 \cdot 10^{14}$	0.995

Application of the isoconversional method is highly recommended by the ICTAC kinetics committee [32] in order to obtain reliable information. The KAS equation (Equation 5) was used for calculation of the activation energy at progressive extents of conversion from the TG data. Figures 5(a) to 5(c) show KAS plots obtained by plotting $\ln(\phi/T_\alpha^2)$ *versus* $1000/T_\alpha$ at different extents of conversion. It was found that all plots exhibited almost linear slopes, with correlation coefficients for the linear regression greater than 0.9797. Table 4 lists the results of the activation energies along with the square of the correlation coefficient. From Table 4, it may be seen that the values of the activation energy were significantly changed with the extent of conversion. This indicates that the thermal degradation reaction mechanism is complex. These results show that the activation energies of RT_1, RT_2 and RT_3 were in the ranges 77.2-235.8 kJ·mol^{-1}, 75.7-224.9 kJ·mol^{-1} and 70.4-196.0 kJ·mol^{-1} for the extent of conversion (α = 0.05-0.95), respectively.

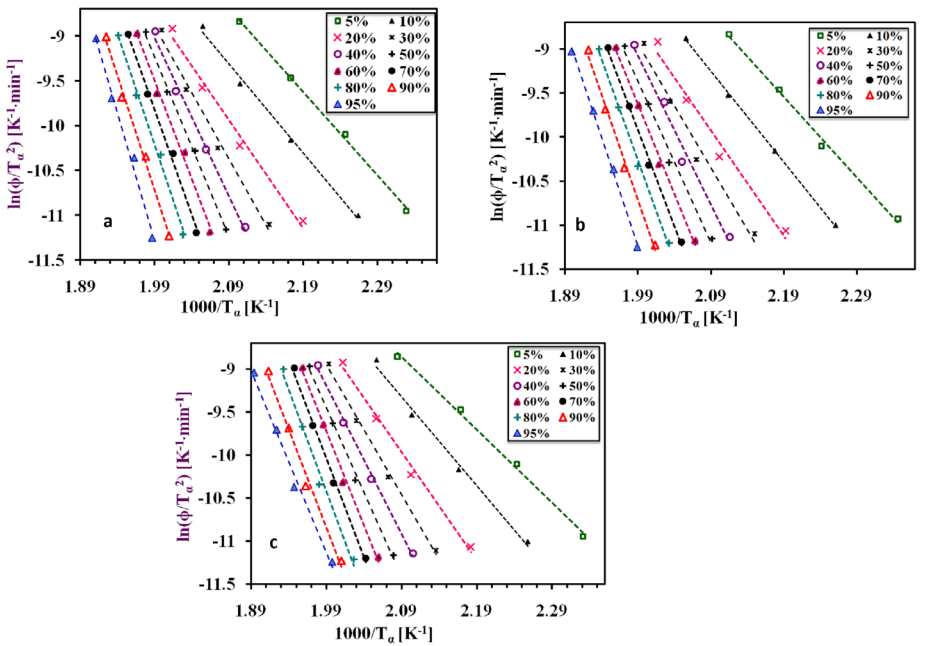

Figure 5. KAS plots for (a) RT_1, (b) RT_2 and (c) RT_3 samples obtained at different heating rate under nitrogen atmosphere

Table 4. The activation energies of RT_1, RT_2 and RT_3 samples for the degradation reaction obtained by the KAS method using TG data

α	RT_1		RT_2		RT_3	
	E_a [kJ·mol^{-1}]	R^2	E_a [kJ·mol^{-1}]	R^2	E_a [kJ·mol^{-1}]	R^2
0.05	77.2	0.9986	75.7	0.9956	70.4	0.996
0.1	82.1	0.9949	85.3	0.9995	85.8	0.9924
0.2	99.9	0.9865	99.3	0.9815	104.4	0.9925
0.3	122.0	0.9879	116.7	0.9797	125.5	0.9958
0.4	146.0	0.9981	140.8	0.9824	143.1	0.9976
0.5	161.7	0.9974	151.6	0.9899	163.2	0.9959
0.6	182.4	0.9942	168.9	0.9961	182.5	0.9923
0.7	194.8	0.9941	182.6	0.9973	191.6	0.9951
0.8	205.9	0.9935	190.5	0.9968	196.0	0.9881
0.9	211.1	0.9993	199.9	0.9937	189.6	0.9891
0.95	235.8	0.9939	224.0	0.9982	184.2	0.9993

The model free kinetic (MEK) software based on the American Society for Testing and Materials (ASTM) E689 method was also used for the calculation of the kinetic parameters. This is based on the theoretical work of the Kissinger method and was applied using the TG data at different heating rates. Figure 6 shows the activation energies for RT_1, RT_2 and RT_3 samples with extent of conversion as calculated by means of the MEK thermo-kinetics software using the ASTM E698 method. The activation energies of the RT_1, RT_2 and RT_3 samples were obtained in the ranges 77.4-236.2 kJ·mol^{-1}, 76.1-224.3 kJ·mol^{-1} and 71.3-196.3 kJ·mol^{-1} for the extent of conversion (α = 0.05-0.95), respectively. The activation energies obtained by this method were in good agreement and consistent with those obtained by the KAS method (Figure 7).

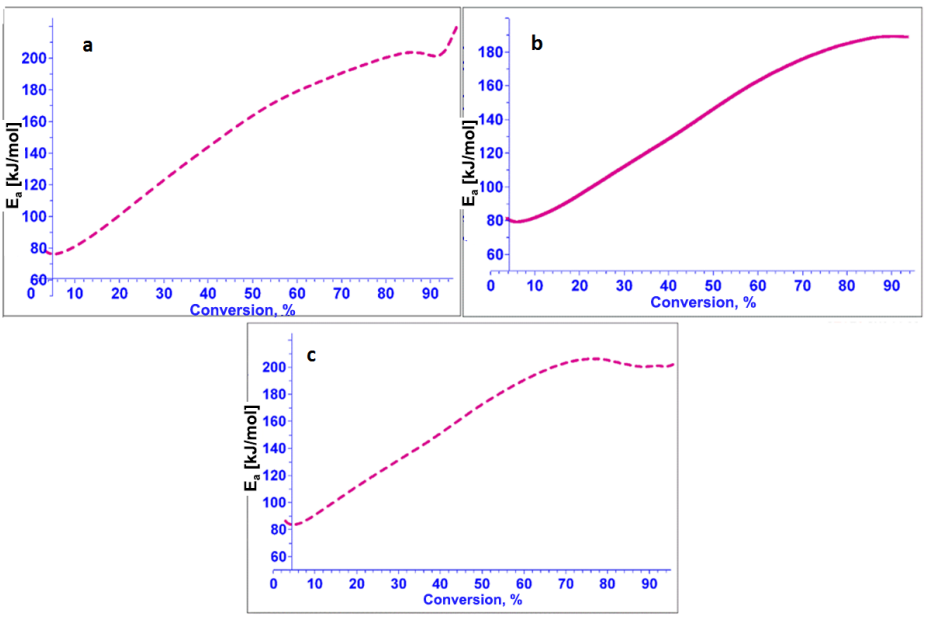

Figure 6. Variation in the activation energy with the extent of conversion for (a) RT_1, (b) RT_2 and (c) RT_3 samples obtained by the MEK software using the ASTM E698 method

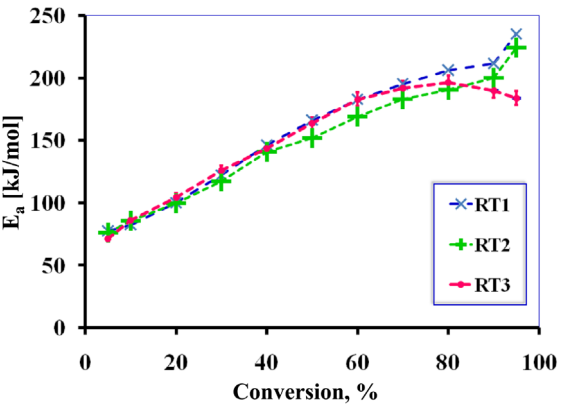

Figure 7. Variation in the activation energy with the extent of conversion for RT_1, RT_2 and RT_3 samples obtained by the KAS method

3.4 Dependence of the activation energy with conversion

The above-mentioned results of the isoconversional kinetic computation of fresh and aged Composition B samples show that the activation energy for thermolysis is dependent on the extent of conversion, as shown in Figure 6. It may be seen that the activation energy for all samples was very low (84 ±2 kJ·mol^{-1}) due to the involvement of two processes, simultaneous evaporation and thermal degradation. Actually, the rates of these processes depend greatly on the temperature and the evaporation at low temperature. At low conversions ($\alpha = 0.05$-0.2), the activation energies were almost the same for fresh and aged samples and comparable with those of pure TNT [8]. Actually, these stages involved less activation energy *i.e.* 84-110 kJ·mol^{-1} than the homolysis of C–NO_2 from the TNT molecule [33]. The density dependent initial degradation path for a density dependent activation energy has been reported to be 104.6 kJ·mol^{-1}, which is lower than the corresponding gas phase uni-molecular reaction barrier (C–NO_2 homolysis). Subsequently, the activation energy has been reported to be around 142.3 kJ·mol^{-1} for the thermal degradation of liquid TNT by means of ESR measurements [34, 35].

At conversions 0.4-0.5, the activation energies were at odds with the literature, and could be the combined effect of the thermal degradation of both TNT and RDX. It has been reported that the activation energy for the thermal degradation of pure TNT is 140 ±10 kJ·mol^{-1} [15, 36]. At conversions of 0.5-0.6, the activation energies were comparable to those obtained from the Kissinger method using the peak temperatures for maximum reaction rate. Overall, the activation energies of the RT_1 and RT_2 samples were found to increase with increasing extent of conversion, while the activation energy of the RT_3 sample was

also found to increase, and to attain a maximum at conversion, $\alpha = 0.9$; thereafter it dropped by 5.0 kJ·mol^{-1}. It has been reported that the thermal degradation of RDX has been attributed to three major steps: vaporization, liquid phase degradation and gas phase degradation. Therefore, the variation in the activation energy for RDX was reported over a wide range, 175-200 kJ·mol^{-1} using different kinetic methods. Maksimov *et al.* [37] have been measured an activation energy of 180.2 kJ·mol^{-1} for the thermal degradation reaction of Composition B (mixture of 65% RDX, 43% TNT and 1% wax) using a DSC method. On other hand, in the present work, the mean activation energies were around 191.7 kJ·mol^{-1} for fresh Composition B, 179.7 kJ·mol^{-1} for 20 y old and 178.6 kJ·mol^{-1} for 32 y old, for the extent of conversion of 0.4-0.95, respectively. The dependence of the activation energy with the extent of conversion from the KAS method was consistent and comparable to those obtained from the MEK thermo-kinetics software using the ASTM E698 method.

3.5 Thermodynamic parameters

The thermodynamic parameters, including the Gibbs free energy for activation ($\Delta G^{\#}$), activation of enthalpy ($\Delta H^{\#}$) and activation of entropy ($\Delta S^{\#}$), for the formation of an activated complex were also determined from the theory of activated complexes [10, 38]. The following general Equation 6 was used:

$$A = \frac{e\chi k_B T_{max}}{h} exp.\left(\frac{\Delta S^{\#}}{R}\right) \tag{6}$$

where $e = 2.7183$ is the Neper number, χ is the transition factor, which is unity for a monomolecular reaction, k_B is the Boltzmann constant ($1.38 \cdot 10^{-23}$ J·s^{-1}), T_{max} is the peak temperature of the degradation reaction rate and h is the Plank constant ($6.626 \cdot 10^{-34}$ J·s^{-1}). The change of the entropy of activation for the formation of an activated complex from the reagent may be calculated from the following Equation 7:

$$\Delta S^{\#} = Rln\frac{Ah}{e\chi k_B T_{max}} \tag{7}$$

since

$$\Delta H^{\#} = E - RT \tag{8}$$

The change of Gibbs free energy for an activated complex formation can be calculated using the well known thermodynamic Equation 9:

$$\Delta G^{\#} = \Delta H^{\#} - T\Delta S^{\#} \quad (9)$$

where $\Delta G^{\#}$, $\Delta H^{\#}$ and $\Delta S^{\#}$ are the Gibbs free energy, enthalpy and entropy of the activation, respectively.

The thermodynamic parameters for the RT_1, RT_2 and RT_3 samples were calculated using Equations 7-9 at different heating rate and the activation energy calculated from the Kissinger method was used. Table 5 lists the results of the thermodynamic parameters such as $\Delta G^{\#}$, $\Delta H^{\#}$ and $\Delta S^{\#}$ for the formation of an activated complex. The value of the Gibbs energy reflects the total energy increase of the system at the approach of the reagents and formation of the activated complex. The value of the activation enthalpy shows the energy difference between the activated complex and reagents. A small difference in this parameter favours the formation of the activated complex due to the potential energy barrier.

Table 5. The thermodynamic parameters of RT_1, RT_2 and RT_3 samples for the degradation reaction obtained from DSC data

ϕ [°C·min^{-1}]	Sample	$\Delta G^{\#}$ [kJ·mol^{-1}]	$\Delta H^{\#}$ [kJ·mol^{-1}]	$\Delta S^{\#}$ [J·(mol·K)$^{-1}$]
2	RT_1	172.7	169.7	2.2
	RT_2	172.1	166.3	–3.6
	RT_3	172.8	183.0	29.3
5	RT_1	172.8	169.7	2.1
	RT_2	172.2	166.3	–3.7
	RT_3	172.6	182.9	29.2
10	RT_1	172.8	169.6	1.9
	RT_2	172.3	166.2	–3.9
	RT_3	172.5	182.9	29.0
20	RT_1	172.9	169.5	1.8
	RT_2	173.4	166.1	–4.0
	RT_3	172.3	182.8	28.9

The $\Delta G^{\#}$ is influenced by two other thermodynamic parameters, namely, enthalpy and entropy of activated complex formation. The $\Delta G^{\#}$ values remained almost constant, which could be attributed to the fact that the $\Delta G^{\#}$ value may have no influence on the degradation mechanism. The results indicate that all values of the $\Delta G^{\#}$ are positive. Therefore, the thermodynamic reactions for degradation are non-spontaneous and need heat to proceed.

The change of entropy for the formation of an activated complex from the reagent reflects how close the system is to its own thermodynamic equilibrium. The low value of entropy for activation means that the system passed through some kind of physical or chemical ageing process. It indicates that the system is brought to a state close to its own thermodynamic equilibrium with low reactivity. On other hand, a high value of the entropy of activation means that the system is brought to a state far from its own thermodynamic equilibrium with high reactivity [39, 40].

4 Conclusions

The thermal degradation behaviour and kinetic parameters of fresh and naturally aged Composition B were studied through non-isothermal DSC and TGA experiments. The results, as suggested by the TGA and DSC data, show that there was no significant change in the thermal stability for the aged samples after prolonged ageing periods. The kinetic parameters were investigated by means of the Kissinger method using the peak temperatures from DSC data obtained at four heating rates (2, 5, 10, and 20 °C·min^{-1}) under a nitrogen atmosphere. The activation energies were also investigated by means of the KAS isoconversional method from the TGA data and were found in the ranges 77.2-235.8 kJ·mol^{-1} for fresh Composition B, 75.7-224.9 kJ·mol^{-1} for 20 y and 70.4-196.0 kJ·mol^{-1} for 32 y old Composition B. These findings show that there was no significant variation in the activation energy for fresh and naturally aged Composition B. The activation energy was also investigated by means of the MEK software using the ASTM E698 method and found to be consistent with those obtained by the KAS method, lying in the ranges 77.4-236.2 kJ·mol^{-1} for fresh, 76.1-224.3 kJ·mol^{-1} for 20 y and 71.3-196.3 kJ·mol^{-1} for 32 y old Composition B. Finally, the thermodynamic parameters such as $\Delta G^{\#}$, $\Delta H^{\#}$ and $\Delta S^{\#}$ were also computed for the thermal degradation using the activated transition theory. The positive values of the E_a, $\Delta G^{\#}$ and $\Delta H^{\#}$ and the low value of $\Delta S^{\#}$ indicate non-spontaneous processes.

Acknowledgement

Authors express their sincere thanks to Dr. Manjit Singh, Distinguished Scientist & Director, for their constant motivation, guidance and fruitful discussion. Our thanks are also due to Dr. P. K. Soni for his kind support for providing thermal analysis to execute this research work.

References

[1] Fouche, F.; Van, S. TNT-based Insensitive Munitions. *Int. Annu. Conf. ICT*, *Proc., 27th,* Karlsruhe, Germany, **1996**.

[2] Huang, H.J.; Dong, H.S.; Zhang, M. Problems and Developments in Composition B Modification Research. *Chin J. Energ. Mater.* **2001**, *9*: 183-186.

[3] Trzciński, W.; Cudziło, S.; Dyjak, S.; Nita, M. A Comparison of the Sensitivity and Performance Characteristics of Melt-Pour Explosives with TNT and DNAN Binder. *Cent. Eur. J. Energ. Mater.* **2014**, *11*: 443-455.

[4] Vuono, C.E. *Military Explosives.* Department of the Army Technical Manual, Washington, D.C., USA, **1990**.

[5] Urbanski, T. *Chemistry and Technology of Explosives.* Vol. 1, Pergamon Press, Oxford, **1964**, pp. 290-300

[6] Akhavan, J. *The Chemistry of Explosives.* 2nd Ed., Cranfield University Press, Swindon, **2004**, pp. 37-39.

[7] Castorina, T.C.; McCahill, J.W.; Forsyth, A.C. Compatibility of Flocculating Agents with RDX/TNT/Comp. B. *J. Hazard. Mater.* **1977-1978**, *2*: 137-142.

[8] Cohen, R.; Zeiri, Y.; Wurzberg, E.; Kosloff, R. Mechanism of Thermal Unimolecular Decomposition of TNT (2,4,6-Trinitrotoluene): a DFT Study. *J. Phys. Chem. A*. **2007**, *111:* 11074-11083.

[9] Pinto, J.; Wiegand, D. The Mechanical Response of TNT and a Composite, Composition B, of TNT and RDX to Compressive Stress: II Triaxial Stress and Yield. *J. Energ. Mater.* **1991**, *9:* 205-263.

[10] Zhang, J.G.; Wang, K.; Niu, X.Q.; Zhang, T.L.; Zhou, Z.N. Theoretical Study of the Decomposition Mechanisms and Kinetics of the Ingredients RDX in Composition B. *J. Mol. Model.* **2012***, 18*(8): 3915-3926.

[11] Colclough, M.E.; Desai, H.; Millar, R.W.; Paul, N.C.; Stewart, M.J.; Golding, P. Energetic Polymers as Binders in Composite Propellants and Explosives. *Polym. Adv. Technol.* **1994**, *5*: 554-560.

[12] An, C.W.; Li, F.S.; Song, X.L.; Wang, Y.; Guo, X.D. Surface Coating of RDX with a Composite of TNT and an Energetic-polymer and Its Safety Investigation. *Propellants Explos. Pyrotech.* **2009**, *34*: 400-405.

[13] Jin, B.; She, N.J.; Gou, X.; Peng, R.; Chu, S.; Dong, H. Synthesis, Characterization, Thermal Stability and Sensitivity Properties of New Energetic Polymers - PVTNP-g-GAPs Crosslinked Polymers. *Polymers* **2016**, *8*: 10-24.

[14] Tuukkanen, I.M.; Brown, S.D.; Charsley, E.L.; Goodall, S.J.; Laye, P.G.; Rooney, J.J.; Griffiths, T.T.; Lemmetyinen, H. A Study of the Influence of the Fuel to Oxidant Ratio on the Ageing of Magnesium-Strontium Nitrate Pyrotechnic Compositions using Isothermal Microcalorimetry and Thermal Analysis Techniques. *Thermochim. Acta* **2005**, *426*(1-2): 115-121.

[15] Long, G.T.; Brems, B.A.; Wight, C.A. Autocatalytic Thermal Decomposition Kinetics of TNT. *Thermochim. Acta* **2002**, *388*: 175-81.

[16] Yao, M.; Chen, L.; Yu, J.; Peng, J. Thermoanalytical Investigation on Pyrotechnic

Mixtures Containing Mg-Al Alloy Powder and Barium Nitrate. *Procedia Eng.* **2012**, *45*: 567-573.
[17] Long, G.T.; Vyazovkin, S.; Brems, B.A.; Wight, C.A. Competitive Vaporization and Decomposition of Liquid RDX. *J. Phys. Chem.* B **2000**, *104*: 2570-2574.
[18] Singh, A.; Soni, P.K.; Sarkar, C.; Mukherjee, N. Thermal Reactivity of Aluminized Polymer-Bonded Explosives Based on Non-Isothermal Thermogravimetry and Calorimetry Measurements. *J. Therm. Anal. Calorim.* **2018**, 1-15.
[19] Chaturvedi, S.; Dave, P.N. A Review on the Use of Nanometals as Catalysts for the Thermal Decomposition of Ammonium Perchlorate. *J. Saudi Chem. Soc*. **2013**, *17*: 135-149.
[20] Sorensen, D.N.; Quebral, A.P.; Baroody, E.E.; Sanborn, W.B. Investigation of the Thermal Degradation of the Aged Pyrotechnic Titanium Hydride/Potassium Perchlorate. *J. Therm. Anal. Calorim.* **2006**, *85*: 151-156.
[21] Kim, Y.; Ambekar, A.; Yoh, J.J. Toward Understanding the Aging Effect of Energetic Materials *via* Advanced Isoconversional Decomposition Kinetics. *J. Therm. Anal. Calorim.* **2018**, *133*: 737-744.
[22] Keith, L. The Development of the Arrhenius Equation. *J. Chem. Educ.* **1984**, *61*: 494.
[23] Kissinger, H. Variation of Peak Temperature with Heating Rate in Differential Thermal Analysis. *J. Res. Natl. Bur. Stand*. **1956**, *57*(4): 217-221.
[24] Akahira, T.; Sunose, T. Method of Determining Activation Deterioration Constant of Electrical Insulating Materials. *Res. Rep. Chiba Inst. Technol. (Sci. Technol.)* **1971**, *16*: 22-31.
[25] Singh, A.; Singh, S.; Sharma, T.C.; Kishore, P. Physicochemical Properties and Kinetic Analysis for Some Fluoropolymers by Differential Scanning Calorimetry. *Polym. Bull.* **2018**, *75*: 2315-2338.
[26] Brill, T.B.; James, K.J. Thermal Decomposition of Energetic Materials. 62. Reconciliation of the Kinetics and Mechanisms of TNT on the Time Scale from Microseconds to Hours. *J. Phys. Chem*. **1993**, *97*: 8759-8763.
[27] Singh, A.; Sharma, T.C.; Narang, J.K.; Kishore, P.; Srivastava, A. Thermal Decomposition and Kinetics of Plastic Bonded Explosives Based on Mixture of HMX and TATB with Polymer Matrices. *Def. Technol.* **2017**, *13*: 22-32.
[28] Singh, A.; Sharma, T.C.; Kishore, P. Thermal Degradation Kinetics and Reaction Models of 1,3,5-Triamino-2,4,6-trinitrobenzene-based Plastic-Bonded Explosives Containing Fluoropolymer Matrices. *J. Therm. Anal. Calorim.* **2017**, *129*: 1403-1414.
[29] Dubikhin, F.F.; Matveev, V.G.; Nazin, G.M. Thermal Decomposition of 2,4,6-Trinitrotoluene in Melt and Solutions. *Russ. Chem. Bull.* **1995**, *44*: 258-263.
[30] Makashir, P.S.; Kurian, E.M. Spectroscopic and Thermal Studies on 2,4,6-Trinitrotoluene (TNT). *J. Therm. Anal. Calorim.* **1999**, *55*: 173-185.
[31] Książczak, A.; Książczak, T. Thermal Decomposition of 2,4,6-Trinitrotoluene During the Induction Period. *Thermochim. Acta* **1996**, *275*: 27-36.
[32] Vyazovkin, S.; Burnham, A.K.; Criado, J.M.; Perez-Maqueda, L.A.; Popescu, C.;

Sbirrazzuoli, N. ICTAC Kinetics Committee Recommendations for Performing Kinetic Computations on Thermal Analysis Data. *Thermochim. Acta* **2011**, *520*: 1-19

[33] Furman, D.; Kosloff, R.; Dubnikov, F.; Zybin, S.V.; Goddard, W.A.; Rom, N.; Hirshberg, B.; Zeiri, Y. Decomposition of Condensed Phase Energetic Materials: Interplay between Uni- and Bi-molecular Mechanisms. *J. Am. Chem. Soc.* **2014**, *136*: 4192-4200.

[34] Rom, N.; Hirshberg, B.; Zeiri, Y.; Furman, D.; Zybin, S.V.; Goddard, W.A.; Kosloff, R. First-Principles-Based Reaction Kinetics for Decomposition of Hot, Dense Liquid TNT from Reax FF Multiscale Reactive Dynamics Simulations. *J. Phys. Chem.* C **2013**, *117*: 21043-21054.

[35] Guidry, R.M.; Davis, L.P. Thermochemical Decomposition of Explosives. I. TNT Kinetic Parameters Determined from ESR Investigations. *Thermochim. Acta* **1979**, *32*: 1-18.

[36] Janney, J.L.; Rogers, R.N. Thermochemistry of Mixed Explosives. *Int. Conf. Thermal Analysis*, *Proc., 7th, Part 2*, Chichester, **1982**, 1426.

[37] Maksimov, Y.Y.; Polyakova, M.V.; Sapranovich, V.F. Thermal Decomposition of Hexogen and Octogen. *Tr. Mosk. Khim.-Tekhnol. Inst. im. Mendeleeva* **1967**, *53*: 73-84.

[38] Turmanova, S.C.; Genieva, S.D.; Dimitrova, A.S.; Vlaev, L.T. Non-Isothermal Degradation Kinetics of Filled with Rice Husk Ash Polypropene Composites. *Express Polym. Lett.* **2008**, 2: 133-146.

[39] Singh, A.; Kaur, G.; Sarkar, C.; Mukherjee, N. Investigations on Chemical, Thermal Decomposition Behavior, Kinetics, Reaction Mechanism and Thermodynamic Properties of Aged TATB. *Cent. Eur. J. Energ. Mater.* **2018**, *15*(2): 258-282.

[40] Vlaev, L.; Nedelchev, N.; Gyurova, K.; Zagorcheva, M.A. Comparative Study of Non-Isothermal Kinetics of Decomposition of Calcium Oxalate Monohydrate. *J. Anal. Appl. Pyro.* **2008**, *81*: 253-262.

Received: October 27, 2018
Revised: September 12, 2019
First published online: September 20, 2019